

# Magnetic behavior of multi-walled carbon nanotube/polypyrrole nanocomposite

Afarin Bahrami<sup>1\*</sup>, Kasra Behzad<sup>2</sup>

## Abstract

Polypyrrole (PPy) and polypyrrole-carboxylic functionalized multiwall carbon nanotube composites (PPy/f-MWNT) were synthesized by in-situ chemical oxidative polymerization of pyrrole monomer on multiwall nanotubes. The effect of the magnetic field intensity from 0 to 10KG on the conductivity of the nanocomposites was studied. The Hall coefficient and Hall mobility of PPy and PPy/ f-MWNT nanocomposite samples with different concentrations of MWNT were measured using the Van der Pauw technique in the same magnetic field range. The mobility decreased slightly with the increasing magnetic field, while the conductivity is dominated by a gradual increase in carrier density. The conductivity values demonstrate the utility of these complex composites as photovoltaic materials. With increasing CNT content, the measured magnetoresistance of the samples became more negative, which supports the fact that the average localization length of the nanocomposite materials is increased, and the charge transport is dominated by the MWNTs.

## Keywords

Polypyrrole, Carbon nanotube, Hall effect, Nanocomposite, Transport properties.

<sup>1</sup> Department of Physics, Islamshahr Branch, Islamic Azad University, Islamshahr, Iran.

<sup>2</sup> Department of Physics, Shahr-e-Qods Branch, Islamic Azad University, Tehran, Iran.

\*Corresponding author: afarin.bah@gmail.com

## 1. Introduction

Conducting polymers are of special concern as they offer numerous electronic advantages compared to their inorganic counterparts, including facile fabrication, control of Fermi levels via doping [1], material flexibility, and relatively cheap manufacturing. There is rising interest in investigating the physical properties of different  $\pi$ -conjugated systems as many oligomers and polymers are encouraging candidates for usage in devices such as field-effect transistors [2, 3], organic light-emitting diodes [4], molecular switches [5], or optical converters [6]. Conjugated polymers can be synthesized in a controlled manner, an important advantage that makes it possible to obtain materials with nano or molecular-scale structures. Due to the rapid development of nanoelectronics, increasing attention is being paid to study the properties of organic and polymeric nanostructures.

Polypyrrole (PPy) is one of the most widely studied organic conducting polymers, and it can be synthesized by electrochemical or chemical oxidation of pyrrole in aqueous media and different organic solvents [7–9]. Electrochemical polymerization is appropriate for the formation of a conducting PPy thin-film; however, it is not a suitable method for mass production. On the other hand, chemical polymerization is a cost-effective, fast, simple, and easily scalable method. The characteristics of prepared conducting polymers are dependent on the synthesis conditions and the additives in the reaction mixture. Carbon nanotubes (CNT) have individual mechani-

cal and electrical properties that are appropriate for synthesizing nanocomposites [8, 10, 11]. Preparation of polymer-CNT nanocomposites is an encouraging approach to integrate CNTs into material of devices in order to benefit from the synergistic effect of the polymer [12, 13]. Polymer-CNT nanocomposites are of special interest for applications in electronic devices, such as antennas and batteries, electromagnetic shielding, electrostatic dissipation, and sensors [14–16]. In a conducting polymer/CNT nanocomposite, the conducting polymer serves as an electron donor, and the CNTs are electron acceptors [17]. This study focuses on combining the complementary properties of carbon nanotubes (CNTs) and polypyrrole (PPy) by employing an in situ chemical route to form a nanocomposite material. The conductivity ( $\sigma$ ), Hall coefficient ( $R_H$ ), Hall mobility ( $\mu_H$ ) and magnetoresistance were measured using a conventional Van der Pauw method with DC current. Experimental results were used to derive these parameters as a function of the magnetic field from 0 to 10 KG for PPy and PPy/MWNT nanocomposites with different percentages of MWNT content. Studying the magnetic properties of conducting polymer can provide more detail about unpaired spins and charge carrying species. In contrast to the importance of charge carrier transport, the Hall mobility and the Hall coefficient of carriers are poorly investigated.

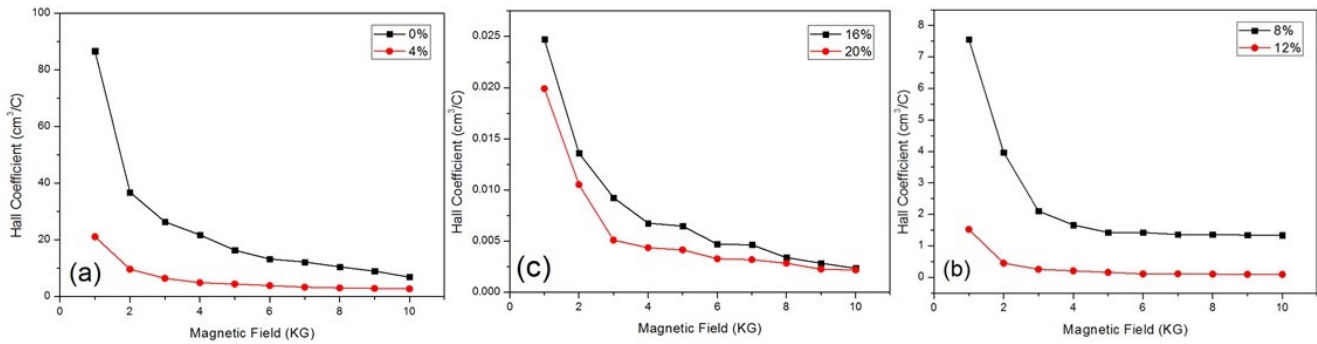


**Figure 1.** The magnetic field dependence of Hall coefficient, (a) for PPy and PPy/MWNT with 4, (b) 8, 12 and (c) 16 and 20 weight percentage of MWNT content.

## 2. Experimental

In this study, the pyrrole monomer (Fluka) was distilled prior to use and stored at 4°C in the absence of light. Carboxylic functionalized multiwalled carbon nanotubes (Nanostructure and Amorphous Materials) and ferric chloride 6-hydrate (HmbG chemical) were of analytical grade and used without further purification. The diameter and length of functionalized multiwalled carbon nanotubes (f-MWNT) were between 10–20 nm and 20 μm, respectively. Polypyrrole coated f-MWNT was synthesized by a chemical in situ polymerization of pyrrole monomer on f-MWNT. The carboxylic MWNTs with different weight ratios were dispersed in distilled water in the presence of SDBS as a surfactant and sonicated for 4 hours to obtain a well-dispersed suspension which enhanced the disaggregation of any nanotube's bundles. Subsequently, a calculated amount of monomer was added to this solution and stirred for 0.5 h. Thenceforth, Ferric chloride 6-hydrates (FeCl<sub>3</sub>.6H<sub>2</sub>O) was added dropwise to the mentioned solution with constant stirring at room temperature, and the mixture was stirred again for another 1 h (the Fe<sup>3+</sup>/pyrrole molar ratio was 2:3). After the reaction, the precipitated PPy/f-MWNTs powders were filtered by the conventional method. Hereafter, the PPy/f-MWNT nanocomposite samples were washed with distilled water and methanol several times until a colorless filtrate was obtained. The resultant powdery product was dried in a vacuum at 40°C for 24 h. The samples were then ground into a fine powder and pressed into very thin pellets. The weight percentages of MWNTs in the PPy/f-MWNT nanocomposite were 0, 4, 8, 12, 16, and 20 wt%.

A Lake Shore Model 7504 Hall effect apparatus was used for magnetic field-dependent measurements in the range of 0 to 10 KG at room temperature. The Hall effect and conductivity were measured using Van der Pauw configuration and conventional DC method with four probes on circular samples with a radius of 13 mm. Silver wires with a diameter of 15 μm were attached to the sample using silver paste. Thenceforward, the measurements were carried out by applying a DC current (10 mA) across two silver wires, and the voltage was evaluated across the other two electrodes. Hall effect measurements were performed under variable magnetic fields from 0 to 10

KG, using an adjustable gap electromagnet, and the current direction was perpendicular to the applied magnetic field.

The samples Hall coefficient ( $R_H$ ) was obtained from the following relation [18]:

$$R_H = \frac{R_{HC} + R_{HD}}{2} \quad (1)$$

where

$$R_{HC} = \frac{t}{B} \frac{V_{31,42}^+(+B) - V_{31,42}^-(+B) + V_{31,42}^-(-B) - V_{31,42}^+(B)}{I_{31}^+(+B) - I_{31}^-(+B) + I_{31}^-(-B) - I_{31}^+(-B)} \quad (2)$$

and

$$R_{HD} = \frac{t}{B} \frac{V_{42,13}^+(+B) - V_{42,13}^-(-B) + V_{42,13}^-(+B) - V_{42,13}^+(-B)}{I_{42}^+(+B) - I_{42}^-(-B) + I_{42}^-(+B) - I_{42}^+(-B)} \quad (3)$$

In the above equations,  $V_{ab,cd}^+$  and  $I_{ab}^+$  denote the positive current is flowing through the  $ab$  contacts, the voltage drop is measured through the  $cd$  contacts, and  $t$  is the thickness of the samples.

## 3. Results and discussion

The Hall coefficient parameter was measured as a function of the applied magnetic field from 0 to 10 KG. The  $B$  dependency of  $R_H$  is shown in Fig. 1. The Hall coefficient is compatible to Eqs. (2) and (3) showing that the  $R_H$  is inversely in proportion to the working magnetic field.

The carrier density can be calculated from the Hall coefficient using the Drude model. Assuming one carrier conduction theory, the carrier concentration,  $P_c$ , and Hall mobility  $\mu_H$  can be calculated by:

$$P_c = \frac{1}{qR_H} \quad (4)$$

and

$$\mu_H = R_H \sigma \quad (5)$$

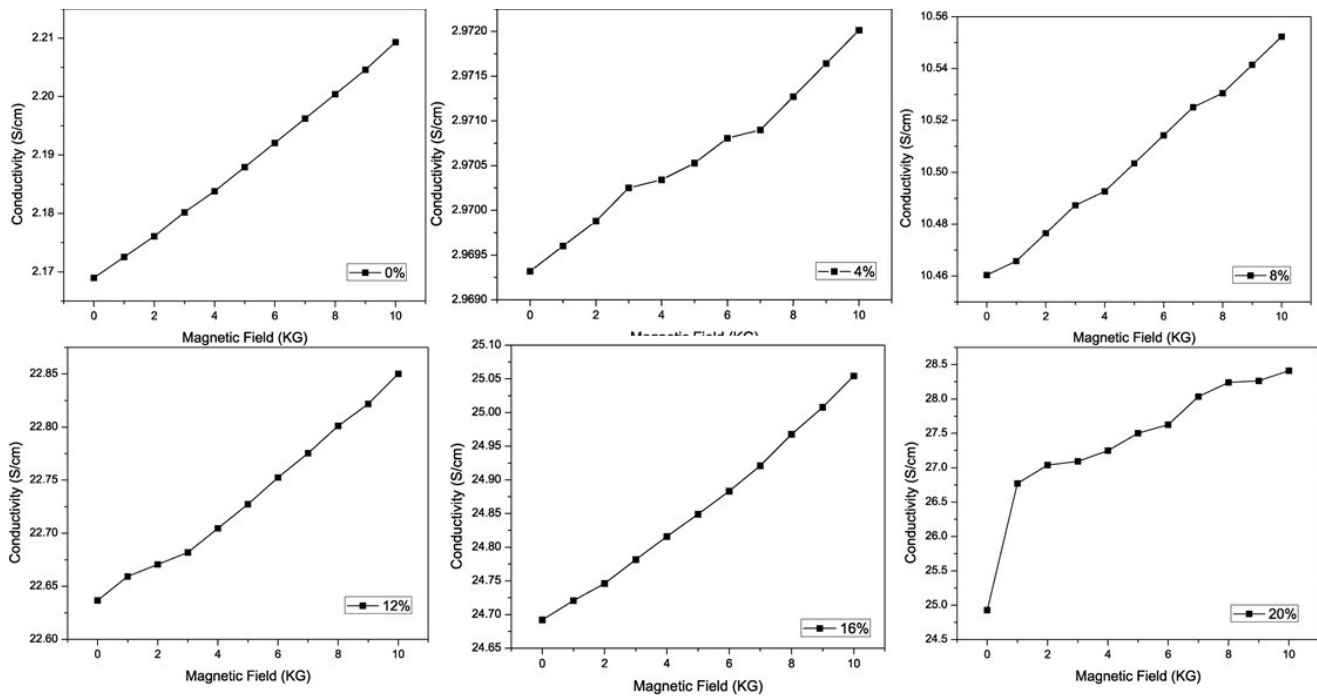


**Figure 2.** The magnetic field dependence of conductivity for PPy and PPy/MWNT with 4, 8, 12, 16 and 20 weight percent MWNT.

where  $q$  is the electronic charge and  $\sigma$  is the conductivity. The increment of the magnetic field causes an increase in the carrier concentration. This can be the reason for the growth in conductivity with the rising applied magnetic field.

Fig. 2 shows the dependence of conductivity on a magnetic field. For all samples, the expansion in magnetic field causes an increase in conductivity, which may be related to a concurrent increase in carrier concentration.

It is important to note that the decrease in Hall mobility with magnetic field, shown in Fig. 3, is because of the increase in free carriers due to the applied magnetic field, in accordance with Eq. (2) and (3), as it was illustrated in Fig. 1.

To clarify the reason for increasing the hole effective mass with the magnetic field, throughout the experiment, the electric and magnetic fields were at right angles to each other. Hence, a rise in the magnetic field would increase carrier effective mass in accordance with the relation  $m_h \propto eB/cw$ , [19] where  $c$  is the light velocity and  $w$  is the carrier rotational frequency. In addition, the electron and hole effective masses in the space of the wave vectors  $k$  are specified as  $m_{hole}^{-1} = \eta^{-2} d^2 E / dk^2$  with  $E = E_v - \eta^2 / (2mh) K^2$  and  $E = E_c + \eta^2 / (2me) K^2$ , where  $E_c$  and  $E_v$  are the conduction and valence band energy levels, respectively. It has been investigated that the applied  $B$  would cause an increase in  $m_h$  that will shift any accessible energy level in the bandgap structure of the material [20]. It has been reported that the applied magnetic field affects the electronic structure by shifting the electron wave functions centers. Moreover, the authors reported that the applied  $B$  enhanced the representative and

the effective density of states of carrier effective masses, the acoustic phonon emission, and the energy separation among different electronic sub bands [21].

#### 4. Magnetoresistance

As the extent of the structural disorder can affect the magnetoresistance (MR), this can be a special applicable probe for determining the scattering process and microscopic transport mechanisms [22]. The room temperature MR results for the 0, 4, 8, 12, 16, and 20wt % CNT/PPy composite powders are shown in Fig. 4. With increasing CNT concentration, the negative contribution to the MR clearly increases, due to the fact that the carbon nanotubes have a long 1D localization length and negative magnetoresistance [23,24].

These results indicate that the MR is a function of CNT loading. It is proposed that the negative magnetoresistance in the hopping conduction mechanism (for example, CNT films [25], CNT pellets [26], disordered  $\text{In}_2\text{O}_3-x$  films [27], and polymer/CNT composites [28]) was also the reason for the dephasing effect of the applied magnetic field on the quantum interference effect among the numerous number of hopping paths. Nanocomposites with different CNT weight percentages show negative MR at 300 K (Fig. 4). The results indicate that electrons are transferred through the nanocable and form a common diffusive system that can be identified through the frame of weak-localization theory, where the effect of interaction between electrons can behave as a perturbation [29]. The magnetoresistance of the hopping regime results from two

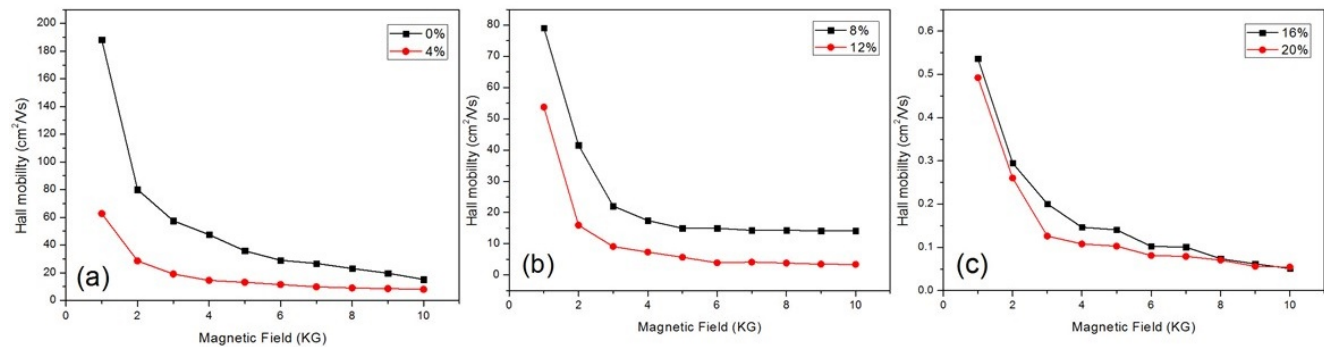


**Figure 3.** The magnetic field dependence of Hall mobility for PPy with different MWNT percentage: 0wt%, 4wt%, 8wt%, 12wt%, 16wt%, 20wt%.

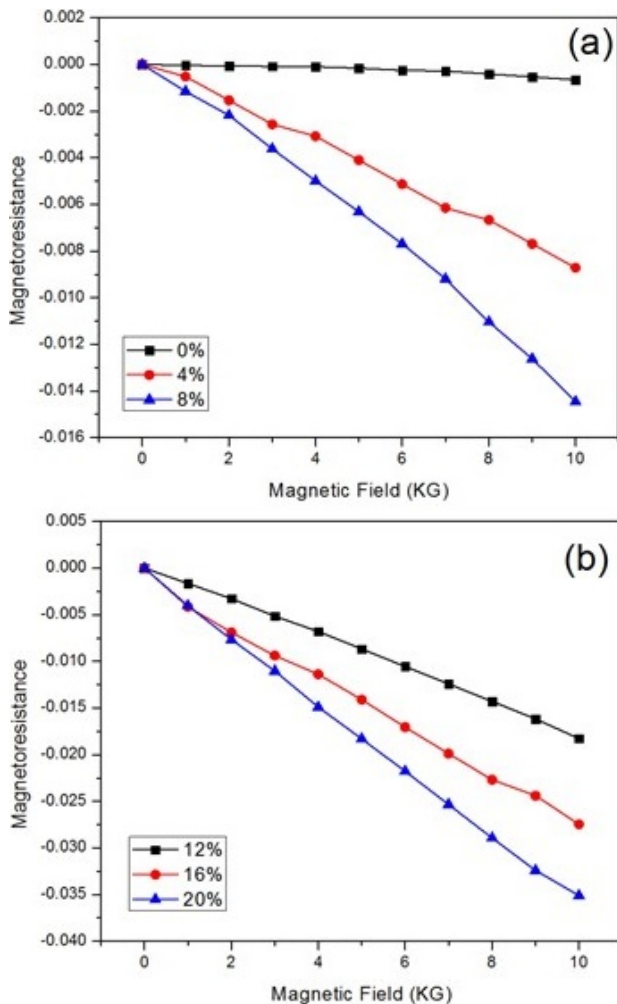


**Figure 4.** The magnetoresistance of pure PPy and PPy with different percentage of MWNT: 0wt%, 4wt%, 8wt%, 12wt%, 16wt% and 20wt%.

effects. Application of magnetic field leads to a contraction of electrons wave functions and decreases the length of average hopping [30]. This is due to the positive magnetoresistance:  $\ln[\rho(H)/\rho(0)] = t \cdot (L_c/L_H)^4 \cdot (T_0/T)^y \propto H^2 \cdot T^y$  where  $t$  is a

constant,  $L_H = (\hbar/eH)^{1/2}$  is the magnetic length, the exponent  $y = 3/2$  for one-dimensional variable range hopping 1D-VRH, and  $y = 3/4$  for 3D-VRH. In addition, if the effect of quantum interference on the variable range hopping is evaluated, it has been reported [31, 32] that the quantum interference modification among many possible hopping paths in the applied magnetic field would result in a negative magnetoresistance:

$[\rho(H) - \rho(0)]/\rho(0) \propto -H^x \cdot T^{-y}$  where  $x = 1$  or 2, [31, 32]  $y = 3/2$  for one-dimensional variable-range hopping and  $y = 3/4$  for three-dimensional variable-range hopping. Recently, a large negative magnetoresistance was described for CNT mat, films, and pellets for weak magnetic fields, which was explained according to the effect of quantum interference [33–35]. The magnetoresistance of PPy/MWNT nanocomposites with a range of MWNT content at room temperature is shown in Fig. 4. The negative MR in PPy is evident; however, it should be considered that PPy has a smaller localization length, i.e., a small average hopping length  $R_h = (3/8)(T_0/T)^{1/4}L_c$  compared to CNTs. From the figure, the magnetoresistance becomes more negative with increased MWNT content. This provides strong evidence for the enhancement of the average localization length of the nanocomposite and the CNTs-dominated charge transfer.

## 5. Conclusion

In this study, PPy and PPy/ f-MWNT were synthesized using chemical in-situ polymerization. The conductivity, Hall coefficient, and Hall mobility of pure PPy and PPy/ f-MWNT nanocomposites were measured using the Hall effect technique at magnetic field intensities from 0.1 to 1T. The mobility was decreased slightly with the increasing magnetic field, while the conductivity was dominated by a gradually increasing carrier density. The conductivity values inspire the usefulness of these nanocomposite samples as photovoltaic materials. The magnetoresistance of the synthesized samples became more negative with MWNT content increment, which is evidence of the increasing localization length of the composites and the CNT-dominated electronic transport.

**Conflict of interest statement:**

The authors declare that they have no conflict of interest.

## References

- [1] A. Tsumura, H. Koezuka, and T. Ando. *Applied Physics Letters*, **49**:1210, 1986.
- [2] H. Chae, J. M. Han, Y. Ahn, J. E. Kwon, W. H. Lee, and B. G. Kim. *Advanced Materials Technologies*, **6**:2100580, 2021.
- [3] J. Wagner, Y. Song, J. Shapiro, and H. E. Katz. *Journal of Materials Chemistry C*, **10**:2149, 2022.
- [4] Y. Xu, Y. Cui, H. Yao, T. Zhang, J. Zhang, L. Ma, J. Wang, Z. Wei, and J. Hou. *Advanced Materials*, **33**:2101090, 2021.
- [5] A. Gupta. *Functional Materials Processing for Switchable Device Modulation*. Elsevier, 1th edition, 2022.
- [6] A. Iwan, W. Pellowski, and K. A. Bogdanowicz. *Energies*, **14**:6186, 2021.
- [7] Z. Morávková, O. Taboubi, I. M. Minisy, and P. Bober. *Synthetic Metals*, **271**:116608, 2021.
- [8] A. Bahrami, Z. A. Talib, E. Shahriari, W. M. M. Yunus, A. Kasim, and K. Behzad. *International Journal of Molecular Sciences*, **13**:918, 2012.
- [9] A. Hussain, A. Dhillon, I. Sulania, and A. M. Siddiqui. *Proceedings of the International Conference on Atomic, Molecular, Optical and Nano Physics with Applications*, **271**:601, 2022.
- [10] Y. Li, J. Wang, H. Duan, L. Han, Q. Jia, X. Liu, S. Zhang, and H. Zhang. *Ceramics International*, **48**:5546, 2022.
- [11] M. Haghgoo, R. Ansari, and M. Hassanzadeh-Aghdam. *Journal of Physics and Chemistry of Solids*, **161**:110444, 2022.
- [12] K. Shehzad, M. N. Ahmad, T. Hussain, M. Mumtaz, A. T. Shah, A. Mujahid, C. Wang, J. Ellingsen, and Z.-M. Dang. *Journal of Applied Physics*, **116**:1, 2014.
- [13] A. Bahrami, A. Sadrolhosseini, G. Mamdoohi, K. Bahzad, and M. Abdi. *Digest Journal of Nanomaterials and Biostructures*, **10**:535, 2015.
- [14] B. De Vivo, P. Lamberti, G. Spinelli, V. Tucci, L. Ver-tuccio, and V. Vittoria. *Journal of Applied Physics*, **116**:054307, 2014.
- [15] H. Song, H. Jeon, D. Im, N. Çakmakçı, K.-Y. Shin, and Y. Jeong. *Carbon*, **187**:22, 2022.
- [16] Q. Ban, Y. Liu, P. Liu, Y. Li, Y. Qin, and Y. Zheng. *Microporous and Mesoporous Materials*, **335**:111903, 2022.
- [17] M. Cochet, W. K. Maser, A. M. Benito, M. A. Callejas, M. T. Martinez, J.-M. Benoit, J. Schreiber, and O. Chauvet. *Chemical Communications*, **16**:1451, 2001.
- [18] D. K. Schroder. *Semiconductor material and device characterization*. Wiley Interscience, 3th edition, 2015.
- [19] C. Kittel. *Introduction to solid state physics*. Wiley Interscience, 1th edition, 1971.
- [20] G. Pan, L. Hu, F. Zhang, and Q. Chen. *Journal of Physical Chemistry Letters*, **12**:3476, 2021.
- [21] W. Xu and C. Zhang. *Applied Physics Letters*, **68**:823, 1996.
- [22] J.-J. Li, Z.-B. Chen, Y.-H. Wang, X.-S. Zhou, L.-Q. Xie, Z. Shi, J.-X. Liu, J.-W. Yan, and B.-W. Mao. *Electrochimica Acta*, **389**:138760, 2021.
- [23] I. Ovsienko, T. Len, I. Mirzoiev, E. Y. Beliayev, D. Gnida, L. Y. Matzui, and V. Heraskevych. *Low Temperature Physics*, **48**:89, 2022.
- [24] I. V. Ovsienko, T. L. Tsaregradskaya, D. O. Shpylka, L. Y. Matzui, G. V. Saenko, U. Ritter, T. A. Len, and Y. I. Prylutsky. *Magnetoresistance of Carbon Nanotubes Filled by Iron*. IEEE, 11th edition, 2021.
- [25] V. Samuilov, J. Galibert, and N. Poklonski. *Perspective of Carbon Nanotubes*. IntechOpen, 1th edition, 2019.
- [26] Y. Yosida and I. Oguro. *Journal of Applied Physics*, **86**:999, 1999.
- [27] O. Faran and Z. Ovadyahu. *Physical Review B*, **38**:5457, 1988.
- [28] K. P. Maity, N. Tanty, and V. Prasad. *Synthetic Metals*, **262**:116345, 2020.
- [29] N. Kang, J. S. Hu, W. J. Kong, L. Lu, D. L. Zhang, Z. W. Pan, and S. S. Xie. *Physical Review B*, **66**:241403, 2002.
- [30] B. I. Shklovskii and A. L. Efros. *Electronic properties of doped semiconductors*. Verlag, 1th edition, 1984.
- [31] V. L. Nguyen, B. Z. Spivak, and B. I. Shklovskii. *Soviet Physics - JETP*, **62**:1021, 1985.
- [32] U. Sivan, O. Entin-Wohlman, and Y. Imry. *Physical Review Letters*, **60**:1566, 1988.
- [33] R. Ghanbari, S. R. Ghorbani, H. Arabi, and J. Foroughi. *Physica C: Superconductivity and its applications*, **548**:78, 2018.
- [34] J.-X. Sui, X.-X. Wang, X.-T. Zhang, W.-P. Han, C. Song, J. Yu, J. q. Chen, H. h. Liu, F. Yuan, and Y.-Z. Long. *Journal of Magnetism and Magnetic Materials*, **498**:166107, 2020.
- [35] A. Robertsam and N. Victor Jaya. *Journal of Nanoscience and Nanotechnology*, **20**:3504, 2020.